2025-1399 IJOI
https://www.ijoi-online.org/

International Journal of Organizational Innovation

THE MAJOR CAUSE OF HIGH-RISE BUILDING FAILURE DURING THE 921 JIJI EARTHQUAKE

Tse-Shan Hsu
Founding President, Institute of Mitigation for Earthquake Shear Banding Disasters
Professor, Department of Civil Engineering, Feng-Chia University, Taiwan R.O.C.
tshsu@fcu.edu.tw

Lin-Yao Wang
Ph.D. and Director, Bureau of Transportation and Public Works, Yunlin, Taiwan, R.O.C.

Abstract

Mat foundations, characterized by their large area and high load-bearing capacity, have traditionally been considered safe by scholars and experts without performing any verification tests. Consequently, cases of tilting and subsidence in high-rise buildings are often attributed to design flaws and inadequate construction practices. In this paper, the authors present a case study examining the tilting and subsidence failures of two high-rise buildings during the Jiji earthquake in 1999, with a focus on the changes in load-bearing capacity of mat foundations during seismic events. The results of this study reveal three key findings: (1) The shear banding effect can easily trigger soil liquefaction; (2) Soil liquefaction can cause a localized loss of load-bearing capacity in the mat foundations of high-rise buildings situated above shear banding zones; (3) When such localized losses occur, buildings may become susceptible to either tilting or subsidence failures. Based on the findings mentioned above, the authors recommend that seismic design codes for mat foundations incorporate provisions to address soil liquefaction induced by the shear banding effect, thereby ensuring the safety of high-rise buildings with mat foundations.

Keywords: high-rise building, mat foundation, shear banding, soil liquefaction.

Introduction

As urban populations expand globally, high-rise buildings have become increasingly prevalent. To address challenges related to load-bearing capacity and uneven settlement, mat foundations are employed due to their considerable weight. Traditional design practices involve establishing a safety factor in accordance with seismic codes and determining the necessary dimensions through limit equilibrium methods (Bowles, 1989). However, this reliance on safety factors often leads to the assumption that mat foundations are inherently safe.

Over the past three decades, many high-rise buildings worldwide have experienced tilting and subsidence failures during seismic events, primarily due to soil liquefaction in the foundation soil (Hsu et al., 2017), resulting in a loss of load-bearing capacity. For instance, the mat foundation of the Haolong Building in Dongshi, Taichung, Taiwan, significantly subsided during the 921 Jiji earthquake, exhibiting localized damage to its first-floor columns (see Figure 1(a)), while overall tilting was observed from the first to the third floors (see Figure 1(b)). Typically, scholars and engineers assess such failures through on-site inspections, often attributing them to design flaws and poor construction practices.

Even experienced professionals may find it challenging to determine the primary cause of a collapse through visual inspections alone. As shown in Figure 2, only one basement column of the Haolong Building experienced significant subsidence during the earthquake, primarily due to a loss of load-bearing capacity in the mat foundation. This subsidence led to fracture failures in three adjacent ground-floor columns at their bases due to arching effects (see Figure 1(b)).

(a) Panoramic view.

(b) Close-up view.

Figure 1. Subsidence failure of the Haolong Building during the 921 Jiji earthquake (Dongshi, Taichung, Taiwan).

Figure 2. Significant subsidence of the mat foundation of the Haolong Building during the Jiji earthquake (Dongshi, Taichung, Taiwan).

Importantly, the failure of the mat foundation, as illustrated in Figure 2, did not occur under normal conditions or during heavy rainfall, indicating that its load-bearing capacity remained intact during these scenarios. However, the foundation failed during the 921 Jiji earthquake, suggesting a temporary reduction in its load-bearing capacity under severe seismic conditions. Generally, the primary reason for localized loss of load-bearing capacity in mat foundations during earthquakes is their positioning atop shear banding zones. Therefore, identifying the shear bands and shear textures surrounding the Haolong Building is crucial for substantiating that the significant subsidence was primarily caused by the shear banding effect during the earthquake.

Shear Band Formation and Shear Banding Effects

Taiwan is situated at the intersection of the Eurasian and Philippine Sea tectonic plates, where ongoing pressure from the latter can destabilize the former. As strain deepens into the plastic range, the Eurasian plate may lose stability and symmetry due to strain softening, leading to localizations of deformations and the formation of shear bands (see Figure 3).

Figure 3. Shear band observed in Zhushan, Taiwan, during the 1999 921 Jiji earthquake (Hsu, 2018).

When conducting a numerical simulation analysis of the shear band shown in Figure 3 using the finite element method, the deformed mesh, including the shear band, is illustrated in Figure 4. Additionally, Figure 5 demonstrates the presence of highly concentrated excess pore water pressure within the shear band.

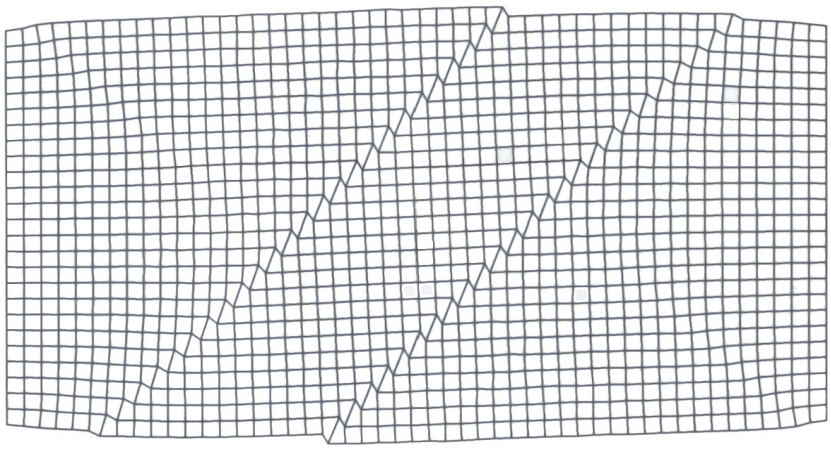

Figure 4. Deformed finite element mesh (Hsu, 1987).

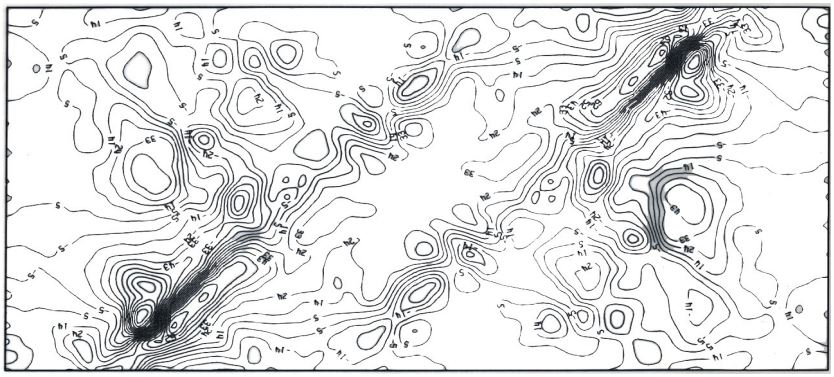

Figure 5. Contours of excess pore water pressures (Hsu, 1987).

Identification of Shear Bands and Shear Textures in the Vicinity of Dongshi District

Figure 6 illustrates the necking phenomenon occurring at the intersection of the plates in the Dongshi and Shigang Districts, and Zhuolan Town of Taichung, Taiwan. It also shows that in the vicinity of the necking area during the 921 Jiji earthquake, several structures were failed, including the Shigang Weir, Pifeng Bridge, Chang Gung Bridge, Dongshi Bridge, Shihwei Bridge, Fengshi Bridge, and Zhuolan Bridge, as well as the Wangchao Building and Haolong Building.

Figure 6 illustrates the necking phenomenon in the tectonic plate at the intersection of the Dongshi and Shigang districts, as well as Zhuolan town in Taichung, Taiwan. In this region, several structures, including the Shigang Weir, six bridges, the Wangchao Building, and the Haolun Building, sustained damage during the 921 Jiji earthquake. The affected bridges include the Pifeng, Chang Gung, Dongshi, Shihwei, Fengshi, and Zhuolan bridges.

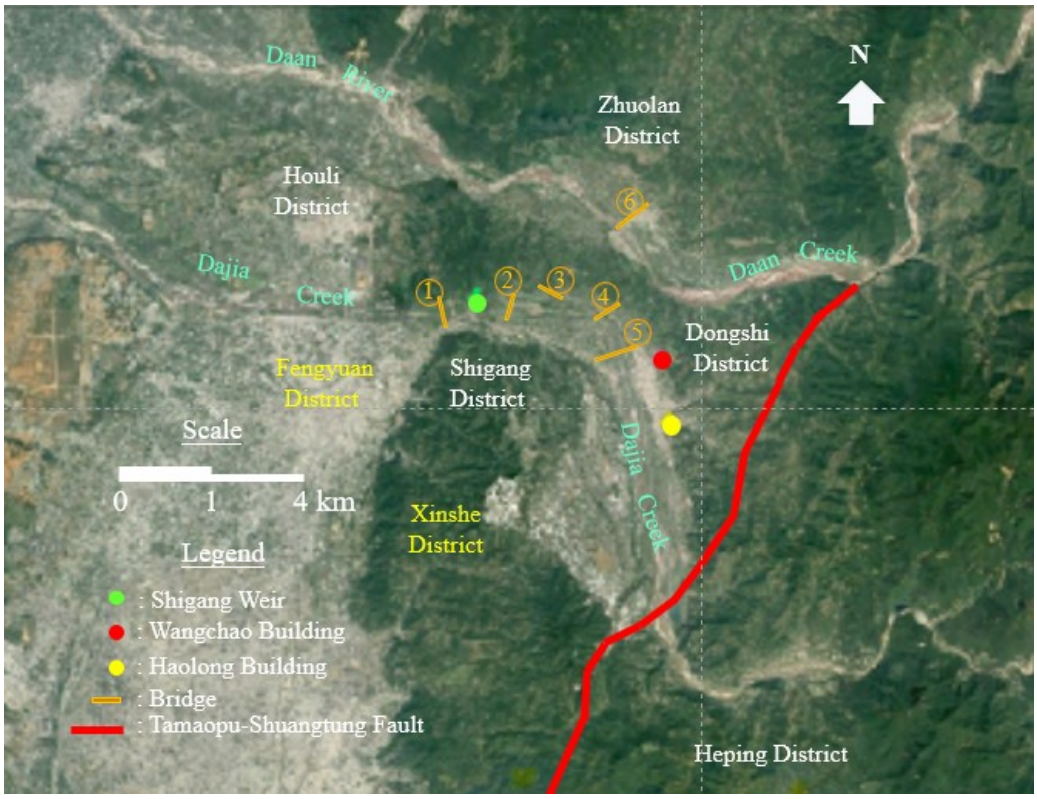

Note: 1: ①: Pifeng Bridge; ②: Chang Gung Bridge; ③: Dongshi Bridge; ④: Shihwei Bridge; ⑤: Fengshi Bridge; and ⑥: Zhuolan Bridge.

Figure 6. Damage to dams, bridges, and buildings in the vicinity of Dongshi during the 921 Jiji earthquake (Background image is taken from Google Earth, 2024).

Figure 7 depicts the Chelungpu Fault zone, which triggered the earthquake. A comparison of Figures 6 and 7 reveals that the foundations of the Shigang Weir, as well as the Pifeng, Chang Gung, Dongshi, Shihwei, and Zhuolan bridges, are embedded within the Chelungpu Fault zone. Consequently, judicial authorities classified the resulting damage as a natural disaster.

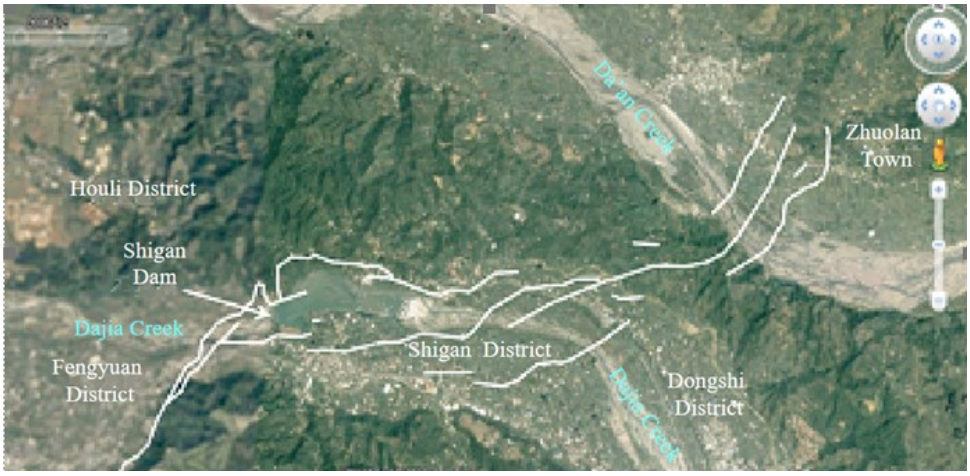

Figure 7. Brittle fracture phenomena in shear banding zones induced by plate necking in Shigang District, Taichung, Taiwan (Hsu et al., 2020).

However, despite experiencing failure during the 921 Jiji earthquake, the Fengshi Bridge, Wangchao Building, and Haolong Building are located outside the Chelungpu Fault zone. The tilting failure of the Wangchao Building resulted in the tragic loss of 28 lives. Consequently, after the earthquake, judicial authorities held the responsible parties accountable for negligence resulting in death, citing design flaws and poor construction practices.

This raises an important question: Is the classification of structural damage as a natural disaster limited to buildings situated within the Chelungpu Fault zone? The answer depends on the presence of shear banding zones and shear texturing zones during the 921 Jiji earthquake.

Figure 8 presents the distribution of GPS horizontal velocity vectors during the earthquake. It is evident that areas with horizontal displacements exceeding 5 meters encompass not only the Chelungpu Fault zone (as shown in Figure 7) but also shear bands and shear textures adjacent to the Damaopu-Shuangdong Fault, as depicted in Figure 8. Therefore, identifying shear bands and shear textures in the Shigang and Dongshi districts is crucial for clarifying whether the structural failure during the 921 Jiji earthquake was attributable to natural disasters.

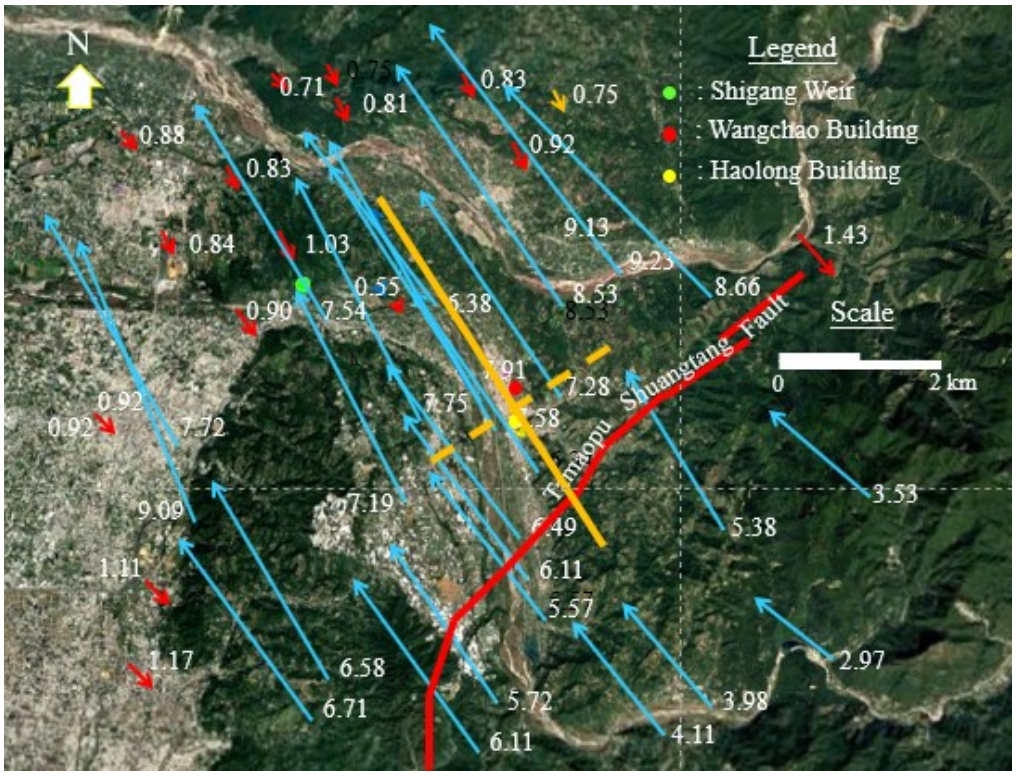

Figure 8. Distribution map of GPS horizontal velocity vectors during the 921 Jiji earthquake (After National Land Surveying and Mapping Center, 2002; Google Earth, 2024).

Identification of Shear Bands in the Vicinity of the Haolun and Wangchao Buildings

Identification of Shear Bands Using GPS Horizontal Velocity Vector Distribution Maps

Figure 8 illustrates the distribution map of GPS horizontal velocity vectors during the 1999 921 Jiji earthquake. This figure reveals the presence of a shear band oriented at N32°W adjacent to the Haolun and Wangchao Buildings, along with a conjugate shear band oriented at N58°E. The horizontal displacement velocity vectors for two neighboring points near these buildings are directed at N32°W, with magnitudes of 7.58 meters and 7.91 meters, respectively. Consequently, during the earthquake, the ground beneath the Haolun and Wangchao Buildings experienced tensile forces that induced a shear band oriented at N58°W.

This tensile force-induced shear band exhibits significant levels of brit-

tle fracture and strain softening. Consequently, in the event of a tectonic earthquake, highly localized excess pore water pressure can lead to soil liquefaction beneath the mat foundations of the Haolun and Wangchao Buildings, compromising the foundations' load-bearing capacity and threatening the stability and safety of the structures.

Figure 9 illustrates the distribution of GPS vertical velocity vectors recorded during the 1999 Jiji earthquake. The data indicates that the vertical displacements of the ground near the Haolong and Wangchao Buildings are 1.43 meters and 1.65 meters, respectively. In contrast, the vertical displacements of the ground to the east and west of these buildings are 0.99 meters and 1.14 meters, respectively.

Thus, during the Jiji earthquake, the eastern ground of both the Haolong and Wangchao Buildings exhibited an uplift relative to the western ground, with a maximum uplift of 0.44 meters at the Haolong Building and 0.66 meters at the Wangchao Building. This uplift phenomenon resulted in the development of shear bands and shear textures, as depicted in Figure 10.

Additionally, the Wangchao Building experienced more significant shear banding and shear texturing effect compared to the Haolong Building during the Jiji earthquake, due to the greater uplift effect on its location.

Figure 9. Vertical GPS velocity vector map during the 921 Jiji earthquake (After National Land Surveying and Mapping Center, 2002; Google Earth, 2024).

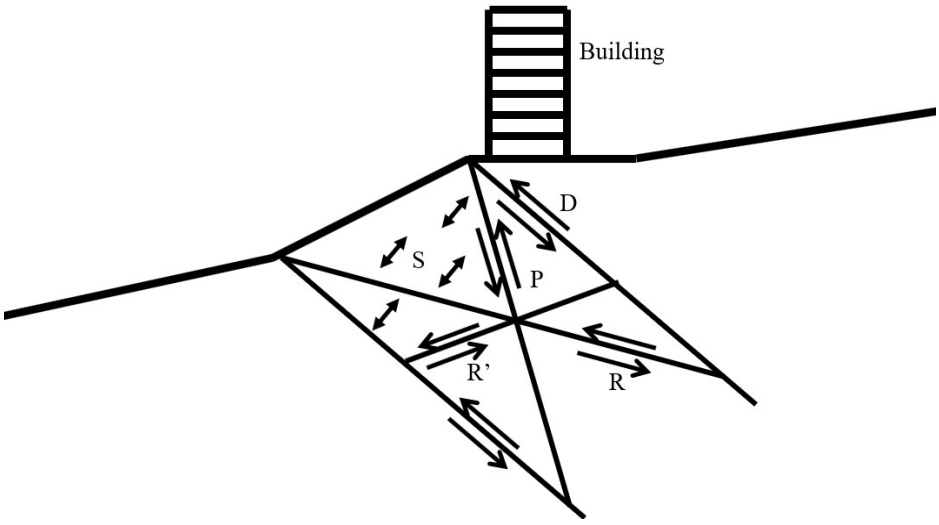

Figure 10. The sites of the Wangchao Building and the Haolong Building are located within shear banding zones.

Identification of Shear Bands and Shear Textures Using Satellite Imagery

1) Identification of shear textures via a N27°E shear band

Using satellite imagery, we identify various shear textures within the overall shear band oriented at N27°E, as illustrated in Figure 11. These textures include a principal displacement shear at N27°E, a thrust shear at N50°E, a Riedel shear at N8°E, a conjugate Riedel shear at N35°W, and a compression texture at N58°W.

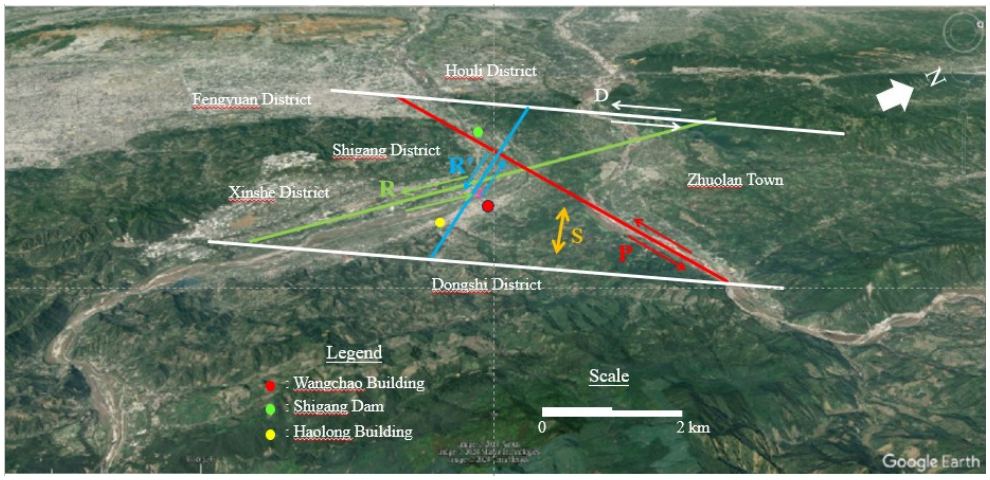

Figure 11. Shear textures identified within the overall width of a shear band oriented at N27°E (Background image is taken from Google Earth, 2024).

2) Identification of shear textures via a N52°E shear band

Similarly, by utilizing satellite imagery, we can identify various shear textures within the overall shear band oriented at N52°E, as depicted in Figure 12. These textures include a principal displacement shear at N52°E, a thrust shear at N74°E, a Riedel shear at N34°E, a conjugate Riedel shear at N1°E, and a compression texture at N33°W.

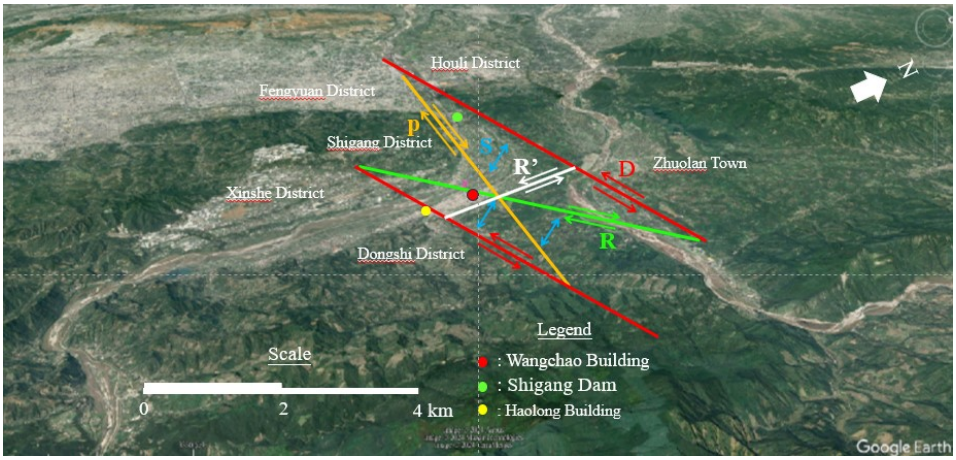

Figure 12. Shear textures identified within the overall width of a shear band oriented at N52°E (Background image is taken from Google Earth, 2024).

3) Identification of shear textures via a N10°W shear band

Utilizing satellite imagery along with shear texture definitions, we also identify shear textures associated with the N10°W shear band, as shown in Figure 13. These textures include a principal displacement shear at N10°W, a thrust shear at N20°E, a Riedel shear at N0°W, a conjugate Riedel shear at N35°W, and a compression texture at N80°E.

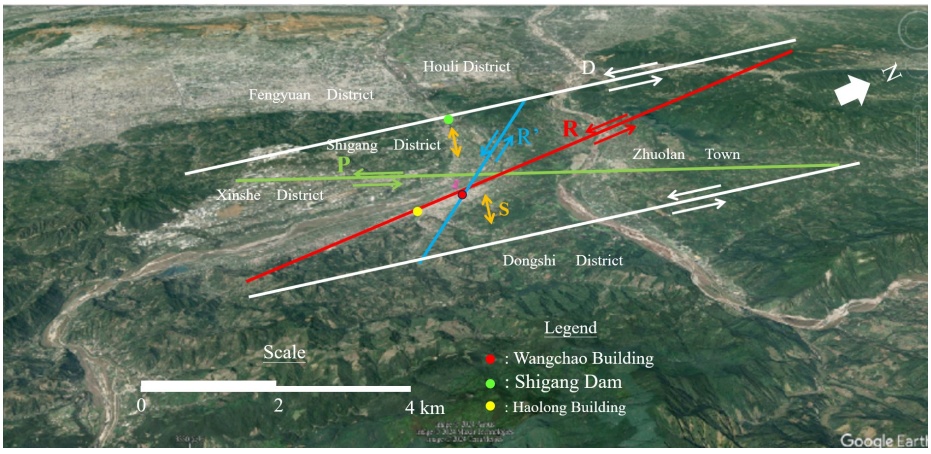

Figure 13. Shear textures identified within the overall width of a shear band oriented at N10°W (Background image is taken from Google Earth, 2024).

Comparison and Discussion

1) Both shear bands and shear textures tend to appear in groups. As shown in Figures 8, and 11 to 13, there are two groups of shear bands with different orientations and 15 groups of shear textures with varying orientations in Dongshi, Taichung, Taiwan. Among these, three groups of shear textures oriented at N0°E, N35°W, and N50°E appear repeatedly. Consequently, there are 14 groups of distinct shear bands and shear textures with varying orientations in Dongshi, Taichung, Taiwan.

2) Under the influence of displacements from these 14 groups of shear bands and textures, Figures 11 to 13 depict the landform deformations induced by shear bands and shear textures in the Dongshi District and its surrounding areas. The most significant deformation is observed at the intersection of the Dongshi and Shigang Districts and Zhuolan Town, where notable necking of the tectonic plates is evident.

3) The severe necking of the tectonic plates, as shown in Figures 11 to 13, is caused by the compression of the Zhuolan Plate along the N0°E or N10°W-oriented shear band toward the Dongshi Plate, while the Shigang Plate is compressed along the N27°E or N34°E-oriented shear band toward the Zhuolan Plate. Due to the differing directions of compression, regions adjacent to the necking area exhibit high levels of brittle fracture in the shear banding zones or the shear texturing zones (see Figure 14), influenced by the displacements of the 14 groups of shear bands and shear textures.

Figure 14. Outcrops of brittle fractures in the zones of shear banding and shear texturing in the riverbed downstream of the Shigang Weir.

4) The shear banding zone extends toward the Shigang Weir, where uplift and tilting effects have caused significant damage to the structure (see Figure 15).

Figure 15. Severe damage to the Shigang Weir resulted from the uplift and tilting effect associated with shear banding.

5) The effects of shear banding and shear texturing resulted in the destruction of the Pifeng, Changgung, Shiwei, Dongfeng, Dongshi, and Zhuolan Bridges (see Figure 6).
6) Figure 6 and Figures 11 to 13 illustrate the 14 shear bands and shear textures responsible for inducing the plate necking effect depicted in Figure 6. During the 921 Jiji earthquake, the uplift and tilting effects of these shear bands and shear textures triggered the subsidence failure of the Haolong Building (see Figures 1 and 2) and the tilting failure of the Wangchao Building (see Figure 16).

Figure 16. Tilting failure of the Wangchao Building during the 921 earthquake (Lian, 1999).

7) The uplift and tilting effects of shear bands and shear textures often trigger soil liquefaction (Hsu et al., 2017). The tilting failure of the Wangchao Building and the subsidence failure of the Haolong Building during the 921 Jiji earthquake were primarily caused by the loss of load-bearing capacity in their mat foundations due to soil liquefaction. The main contributor to soil liquefaction is the strain-softening of the soil within the shear bands beneath the mat foundations, combined with highly concentrated excess pore water pressure in localized areas of groundwater within shear bands or shear textures. Consequently, soil

particles within the shear bands vary in size, from small to large, and can be expelled upward along with groundwater through pipes formed by the interconnected pore spaces within the shear bands or shear textures.

8) When the failures of the Shigang Weir and the six bridges depicted in Figure 6 were attributed to a natural disaster during the 921 Jiji earthquake, the tilting failure of the Wangchao Building should also be considered a consequence of a natural disaster. This is particularly relevant since the building's seismic design codes did not include provisions to fortify against shear banding effect.

Conclusions and Recommendations

This paper presents findings from numerical simulation analysis of shear bands formed in a tectonic plate, identifying shear bands and shear textures induced by necking phenomena at the junction of Dongshi and Shigang Districts, and Zhuolan Town. These findings lead to the following conclusions:

1) The Dongshi District in Taichung, Taiwan, is situated near 14 different shear bands and shear textures, which significantly contribute to observable uplift and tilting effects on dams, bridges, and buildings.

2) The damage to dams and bridges caused by the uplift and tilting effects of shear bands and shear textures during the tectonic earthquake has been classified by judicial authorities as a result of natural disasters. However, the uplift and tilting failure of the Wangchao Building in Dongshi District, Taichung, Taiwan, under the same shear band and shear texture effects during the same seismic event was determined by the authorities to be due to design flaws and poor construction practices.

3) During the 921 Jiji earthquake, the tilting failure of the Wangchao Building and the subsidence of the Haolong Building were attributed to the loss of load-bearing capacity in part of their mat foundations due to soil liquefaction. This liquefaction resulted from plastic strain softening in the shear banding and shear texturing soils, exacerbated by highly localized excessive pore water pressure within the groundwater in these areas.

Based on the three conclusions drawn from this study, the authors recommend that seismic design codes for various structures should not only emphasize fortification against ground vibrations but also incorporate meas-

ures to address the effects of shear banding and shear texturing. This dual approach aims to prevent damage to structures caused by shear banding or shear texturing during earthquakes. Furthermore, it is hoped that this research will aid judicial authorities in accurately identifying the causes of structural failures in accordance with the actual circumstances following any disaster.

References

Bowles, Joseph E., *Foundation Analysis and Design*, 4th Edition, McGraw-Hill Book Co. pp. 436-470, 1989.

Google Earth, Website: http://www.google.com.tw/intl/zh-TW/earth/, 2024

Hsu, Tse-Shan, *Capturing Localizations in Geotechnical Failures*, Ph.D. Dissertation, Civil Engineering in the School of Advanced Studies of Illinois of Technology, 1987.

Hsu, Tse-Shan, "The Major Cause of Earthquake Disasters: Shear Bandings," A Chapter in *Earthquakes-Forecast, Prognosis and Earthquake Resistant Construction*, Edited by Valentina Svalova, IntechOpen, pp. 31-48, 2018.

Hsu, Tse-Shan, Chang-Chi Tsao, and Chihsen T. Lin, "Localizations of Soil Liquefactions Induced by Tectonic Earthquakes," *The International Journal of Organizational Innovation,* Vol.9, No. 3, Section C, pp. 110-131, 2017.

Lian, Yang-Wang, *Cracks in the Earth: Aerial View of the Chengkungpu Fault*, Flytiger Culture Enterprise Co., Ltd., 1999.

National Land Surveying and Mapping Center, Ministry of Internal Affairs, R.O.C., Taiwan, 921 Jiji Earthquake Survey Records, 2002.